STAR
Research Journal

Available online at www.starresearchjournal.com (Star International Journal)

PHYSICS

MORPHOLOGICAL CHARACTERIZATION ON THE NANO STRUCTURE OF SILVER OXIDE USING XRD TOOLS AND COMPUTATIONAL METHODS

R. VISHNUPRIYA[1] & Dr. M.K. MURALI[2]

[1]*Ph.D Scholar, Department of Physics, J.J. College of Arts and Science, Pudukkottai, Tamilnadu, India.*
[2]*Assistant Professor & Head, Department of Physics, J.J. College of Arts and Science, Pudukkottai, Tamilnadu, India.*

Abstract

In this work, the nano silver oxide (Ag_2O) was prepared in the shape of thin-film using Electron beam evaporation method to examine the structural and morphological properties, the fabricated material was annealed at 100º, 200º and 300º C temperatures respectively. The structural modifications and phase transitions were keenly observed at different annealed temperatures and the associated properties were determined by knowing the parameters. Theoretically predicted structures for Ag_2O were displayed and they were validated with experimentally obtained structure. The XRD peaks from respective planes were observed and they were found to be well organized on different phase transitional structures. The morphological views at phase transitions were observed and the cause of modification of physical and chemical properties was keenly monitored. The fundamental lattice type of silver was viewed and the change of structure with respect to interstitial of O at lattice points was clearly displayed and the FCC face of Ag_2O was demonstrated. The existence of micro-strain on lattice site was found and the effect of crystal reciprocity (BCC) was evaluated.

Keywords: Ag_2O, XRD, FCC, micro-strain and crystal reciprocity.

1. INTRODUCTION

The crystalline solid materials always existed in nature and each and every crystal having specific properties for the societal applications. The fundamental physical and chemical properties can be studied from the crystallographic structure [1]. The macro as well as nano structured crystals are generally modified its crystal construction unexpectedly with the aid of the temperature and pressure. It is also varies with the rate of change of temperatures directly, strongly and irreversibly which resulting an irregular change of material properties [2]. Obviously, the structural transition always taking place according to the reinforced temperature improvement in the materials. The occurrence of nano crystalline phase transitions are having great attention due to its purposive defect generated in the material for the special applications. These Martensitic phase transition is a solid-to-solid phase transition where the low-range diffusion of atoms are taking place by which the lattice or molecular structure gets modified. It always achieved by the applications of annealing

process. The phase transitions can be clearly viewed and studied by observing significant dislocations and twinning in the parent phase [3]. In addition to that, the phase transitions are also accomplished by reducing the macro structure to nano structure form [4]. For example, when the Ag_2O is reduced from macro level to the nano level, the lattice structure is transformed from simple cubic to face centered cubic [5].

In silver oxide crystals, the strong forces of attraction existed between silver and O atoms which make cubic lattice system whereas when it is reduced to the nano level material, the crystal getting strained mechanically and the forces of attraction between silver and O atoms become much higher and rearranging the crystal lattice to FCC form. The literatures showed the appearance of phase transitions in silver oxide crystals [6-7]. After making thorough investigation, it was found that, no work related to analyze the crystal phase transitions at the nano level of materials. In this work, the morphological studies were carried out on XRD and theoretical results to solve the phase transitions taking place in nano Ag_2O material.

2. EXPERIMENTAL METHODS

Here the nano Ag_2O material thin film was prepared by Electron beam evaporation technique based on vacuum related techniques [8-9], which is still widely used in the laboratories and in industries for depositing metals and metal alloys. Thin films of Ag_2O were prepared by EB technique using a HINDHI-VAC vacuum unit (model: 12A4D) fitted with electron beam power supply (model: EBG-PS-3K). Well degreased microscopic glass plates have been employed as the substrate.

3. COMPUTATIONAL METHODS

In this case, the Ag_2O material was characterized by performing Gaussian computational calculations in MAC 3 computer. The HF method was used to compute all the parameters at the temperatures range from100º to 300ºC with 6-311G (d,p) basis set. The computer simulation is effective tool to illustrate interaction between nano atoms for producing special characteristics. This computational model is predominantly suitable for metal oxide semiconductor systems [10]. The computed base lattice was reduced to nano level and the calculations were carried out.

TABLE 3
CALCULATED FREQUENCIES OF Ag_2O IN REDUCED NANO LEVEL

S. No.	Calculated Frequency(cm^{-1})			Vibrational assignments
	FT-IR	IR intensity	Raman intensity	
1	1047	1.33	74	(Ag-O)υ asym
2	1046	1.8	2.3	(Ag-O)υ asym
3	1039	4.1	26.9	(Ag-O)υ sym
4	441	47	1.6	(Ag-O)υ sym
5	434	98	6.6	(Ag-Ag)υ sym
6	421	32	1.4	(Ag-Ag)υ
7	410	24	2.6	(Ag-Ag)υ
8	410	52	1.8	(Ag-Ag)υ
9	377	14	1.5	(Ag-Ag)υ
10	358	91	2.5	(O-Ag-O) δ
11	348	16	4.8	(O-Ag-O) δ
12	342	32	1.18	(O-Ag-O) δ
13	340	77	1.3	(O-Ag-O) δ
14	318	5.7	1.0	(O-Ag-O) δ
15	214	55	2.2	(O-Ag-O) γ
16	155	117	1.4	(O-Ag-O) γ
17	127	9.12	1.9	(O-Ag-O) γ
18	122	2.8	1.1	(O-Ag-O) γ
19	109	7.5	1.2	(O-Ag-O) γ
20	108	1.0	1.0	(Ag-Ag) δ
21	101	2.5	1.3	(Ag-Ag) δ
22	92	1.44	1.1	(Ag-Ag) δ
23	80	3.7	1.1	(Ag-Ag) γ
24	77	3.7	1.1	(Ag-Ag) γ
25	74	0.5	1.2	(Ag-Ag) γ

vs; very strong, s; strong, m; medium, w; weak, vw; very weak. υ; stretching, δ; in plane bending: γ-out of plane bending

3. RESULTS AND DISCUSSION

3.1 XRD CHARACTERIZATION

The electronic scanning physical view of prepared Ag_2O thin film was displayed in the Figure 1 where the clear plane view of silver oxide particles can be seen. The amalgamation of oxygen in silver sites was appeared with rather fluctuated surface was identified in the Figure. In order to study the morphological characteristics, the XRD pattern for prepared Ag_2O films were recorded with annealing temperatures of 100º, 200º and 300º C and were publicized in Figure 2. The pattern was observed in each and every temperature separately and the peaks were obtained with sufficient intensity. Particularly, at 100º, the diffraction peaks at 38º, 43º, 54º and 63º were observed and have been assigned to (200), (211), (220) and (311) inter planes of crystal correspondingly. According to the JCBDS data, the XRD blueprint revealed that, the Ag_2O crystal was found to be constructed by face-centered-cubic (fcc) lattice and the observation was supported by the literatures [11-13]. In order to examine the phase transition, the XRD pattern for Ag_2O at 200º and 300º C were also recorded as in 100º, where all the peaks were obtained with maximum intensity and these peaks was identified to be shifted. The dislocated peaks were observed at 38.5º, 43.5º, 54.5º & 63.5º for 200º C and at 39º, 44º, 55º and 64º for 300º C respectively. Here, for every annealing temperature of 100º C, the peaks were found to be shifted up to 0.5º and this may be due to the phase transitions taking place by the enforcement of annealing temperatures. Hence, other than the peak from (200) plane, all the signals were appeared with minimum intensity and the functional temperatures influencing the morphological characteristics. Generally, the phase transitions taking place between the phases of the material whereas here, the transitions were observed within the material morphology canonically. This effect was pronounced in the crystal in terms of micro strain which was generated well deep into the crystal and this arrangement was found to be affected the reciprocal lattice; BCC within the FCC of Ag_2O. The observed reciprocity phase transitions effect was supported by the previous works [14-15].

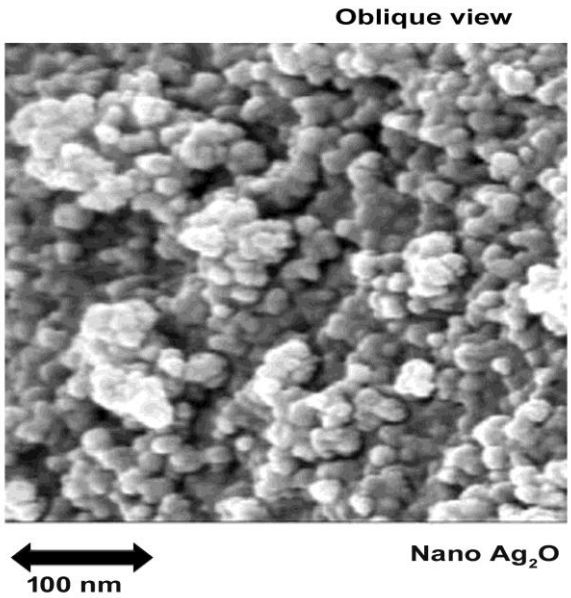

FIGURE 1
ELECTRONIC SCANNING PHYSICAL VIEW OF PREPARED Ag_2O THIN FILM

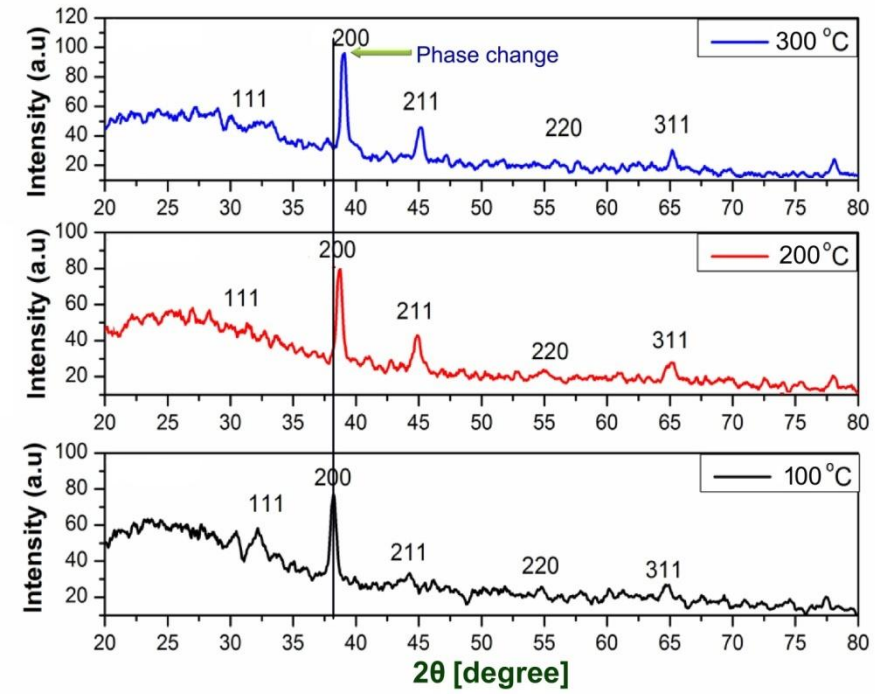

FIGURE 2
XRD PATTERN FOR Ag_2O

In the interplane part of (200), the peak intensity was identified to be increased with annealing temperature of the material. From the observation, it was ensured that, the crystalline character of Ag_2O is significantly enhanced from 200º to 300º C. Besides the diffracted Bragg signals from face centered cubic (fcc) lattice planes of Ag_2O nanocrystals, accompanying unassigned apex were also established and these peaks showed the other phases of exterior of the nano metal oxide particles. From the above observation, it was clear that, crystalline quality of Ag_2O is greatly enhanced by the annealing process and the generation of microstrain within the crystal system produced the reciprocal crystal effect. The associated XRD parameters of Ag_2O were depicted in the Table 1.

TABLE 1
XRD STRUCTURAL PARAMETERS OF Ag_2O THIN MATERIAL DEPOSITED WITHOUT OXYGEN ATMOSPHERE

Annealing temperature (ºC)	Position (2θ)	(hkl)	a (Å)	Strain (βcosθ/4)	Particle size(nm)	Thickness (µm)
Room temperature	--	--	4.712	--	--	0.78
100	38.0	200	4.811	0.0037	32.14	0.69
200	38.5	200	4.900	0.0049	31.54	0.61
300	39.0	200	4.988	0.0061	30.36	0.54

The physical and chemical property of the nano particle always depends upon the particle size which can be calculated from observed FHWHM. The present hetero nuclear nano material was made up of couple of Ag and O atoms. Regularly the nano metal oxide crystal, particularly, it was formed by alternative atoms of Ag and O in the form of chain which is connected to the chain at perpendicular direction on another interplane. Thus, the Ag_2O crystal structure was constructed by linking of chain of consecutive Ag and O in FCC frame. Here, the Figure 3 showed the theoretically predicted crystal structure in which the Ag atoms at FC position were surrounded by O atoms. Whereas, in its reciprocal BCC lattice, O atom is at BC position and it is surrounded by Ag atoms. In above all, the effective crystal system was fabricated by FCC lattice. The

physical property of entire crystal system was changed little bit the application of annealing temperature.

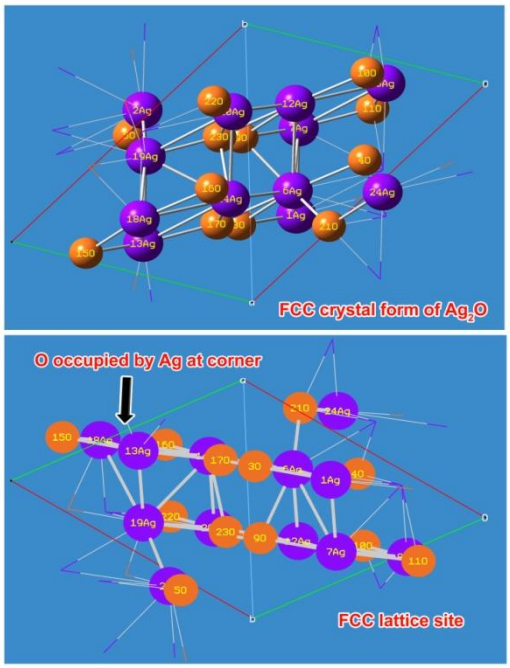

FIGURE 3
THEORETICALLY PREDICTED CRYSTAL STRUCTURE IN WHICH THE Ag ATOMS AT FC POSITION WERE SURROUNDED BY O ATOMS.

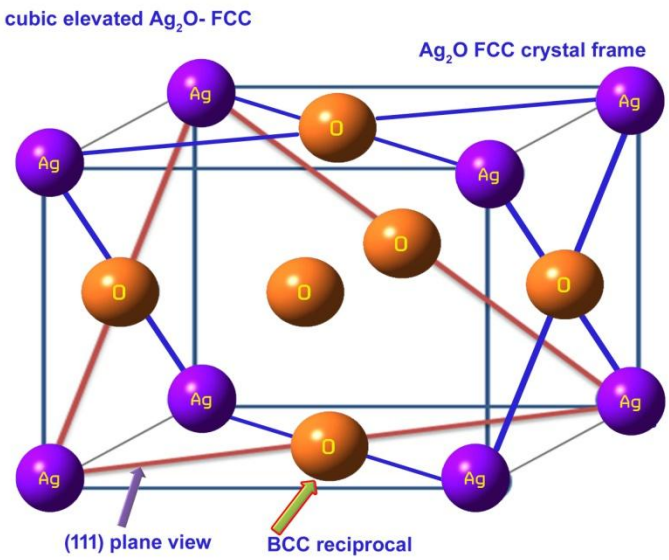

FIGURE 4
PREDICTED MOLECULAR FCC SYSTEM

Another predicted molecular FCC system was depicted in the Figure 4 where the clear picture of FCC lattice and reciprocal system; BCC can be seen. The effect of temperature was observed only in BCC lattice and not in FCC crystal form which is due to the standard structure formation of FCC. The ratio of Ag and O was found to be 2:1 and 1:2 in FCC and BCC respectively. This was confirmed in the reciprocal of XRD peaks arranged in spectrum.

According to the XRD, the average grain size of Ag_2O was calculated by Scherrer's equation from FHWHM,

$$D = k\lambda/(\beta \cos\theta),$$

here D is known as grain size, β called full width at half maxima, θ was the diffracted angle, and λ was found to be wavelength (1·5406 Å). The disparity of particle size and thickness of Ag_2O at different annealing temperatures were obtained in the Figure 5.

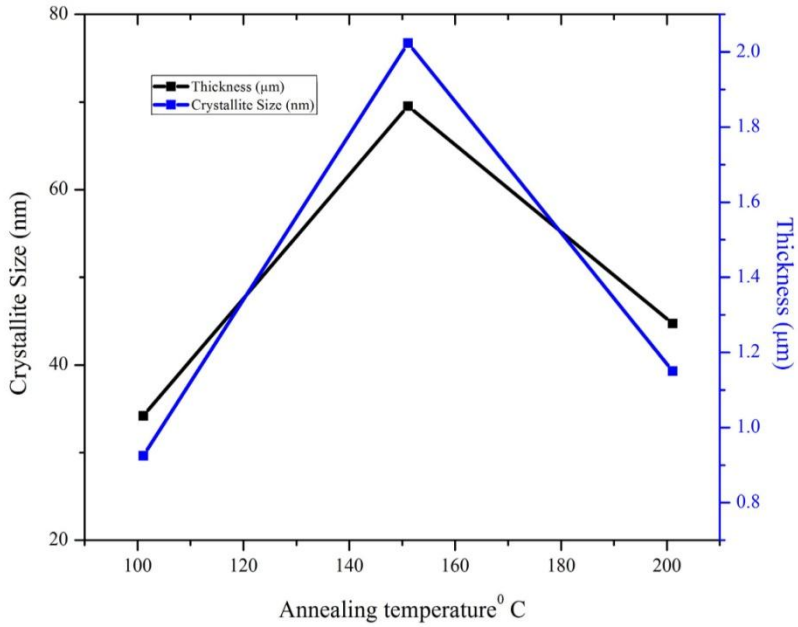

FIGURE 5
THE DISPARITY OF PARTICLE SIZE AND THICKNESS OF Ag_2O AT DIFFERENT ANNEALING TEMPERATURES

The lattice parameter a of the Ag_2O material at room temperature was calculated using the formula in the face centered cubic crystal structure. For the cubic crystal system, the lattice parameter c was related to d with the subsequent equation [16]

$$\frac{1}{d^2} = \frac{h^2 + k^2}{a^2} + \frac{l^2}{c^2}$$

$$2d_{hkl} 2 \sin\theta = m\lambda$$

where h, k, and l are the indices of lattice planes (miller indices), generally, a and c are the lattice constants, d_{hkl} was the distance between two successive planes (m=1) with lattice plane index (hkl).

The crystal parameter values such as strain (ϵ), dislocation density (δ) and number of crystallites (N) were calculated by standard formula [17],

The strain produced in the crystal ε was calculated by the following relation:

$$\varepsilon = (\lambda/D\cos\theta)-(\beta/\tan\theta)$$

The calculated strain was found to be 0.0037, 0.0049 and 0.0061 at consecutive temperatures respectively and it was getting elevated with respect to the temperatures. Since the reduction of particle size taking place with respect to annealing temperature, the proportionate crystal strain was generated.

The dislocation density (δ) of thin films with cubic structure has been calculated by the formula

$$\delta = 15\,\varepsilon/aD$$

The dislocation density was also elevated with respect to the temperature which causing the production of O vacancies among the crystal sites. Using grain size (D) and film thickness (t), the number of crystallites N can be estimated using the relation

$$N = t/D^3 / \text{ unit area}$$

The crystal size was reduced further due to the temperatures and it may be continued along with the temperatures. Similarly, the quality of the crystal was found to be improved from100º to 200º C, and it was also observed that, the electro-optical properties of Ag_2O were really enhanced. The crystallite size, extension coefficient, absorption coefficient, band gap and refractive index at different temperatures were specified in the Table 3. Here, the optical band gap was increased slightly due to the temperatures as it was expected which also affecting the optical characteristics of the nano material. Similarly, the refractive index also increased considerably which was by the effect of temperatures. This increment in such material enhanced the velocity of light in ordinary as well as extraordinary modes and the second harmonic generation process was also induced for the application of laser. The absorption and extinction coefficients were found to be varied in dissimilar manner which was due to the effect of micro strain generated in

the lattice site.

TABLE 2
OPTIMIZED GEOMETRICAL PARAMETERS FOR Ag_2O ANNEALED AT 100º-300º C

Geometrical Parameters	HF/6-311+G(d,p)		
	100ºC	200ºC	300ºC
Bond length(Å)			
Ag1-O3	2.2773	2.2391	2.1990
Ag1-O5	2.2773	2.2391	2.1990
Ag2-O4	2.2406	2.2030	2.1636
Ag2-O5	2.1956	2.1588	2.1201
Ag2-O11	2.8514	2.8036	2.7534
O3-Ag2	2.1956	2.1588	2.1201
O4-Ag6	2.2407	2.2031	2.1637
Ag7-O9	2.8514	2.8036	2.7534
Ag7-O11	2.2270	2.1896	2.1505
Ag8-O10	2.2270	2.1896	2.1505
Ag8-O11	2.2993	2.2607	2.2203
O9-Ag12	2.2951	2.2566	2.2162
O10-Ag12	2.2951	2.2566	2.2162
Bond angle(º)			
O3-Ag1-O5	123.993	121.882	119.782
O4-Ag2-O5	132.644	130.385	128.139
O4-Ag2-O11	108.241	106.397	104.564
C5-Ag2-O11	32.040	31.494	30.952
Ag1-O3-N6	98.080	96.410	94.749
Ag2-O4-C6	83.235	81.817	80.408
Ag1-O5-Ag2	98.074	96.404	94.743
O3-Ag6-O4	132.639	130.381	128.134
O3-Ag6-O9	32.039	31.494	30.951
O4-Ag6-O9	108.239	106.396	104.563
O9-Ag7-O11	149.065	146.527	144.003
O10-Ag8-O11	98.750	97.068	95.396
Ag6-O9-Ag7	87.740	86.246	84.760
Ag6-O9-Ag12	67.670	66.518	65.372
Ag7-O9-Ag12	84.404	82.966	81.537
Ag8-O10-Ag12	138.931	136.565	134.213
Ag2-O11-Ag7	87.739	86.245	84.759
Ag2-O11-Ag8	67.671	66.519	65.373
Ag7-O11-Ag8	84.404	82.967	81.537
O9-Ag12-O10	98.740	97.059	95.386

3.2. MULLIKEN CHARGE PROFILE

The theoretically predicted charge structure was presented in the Figure 6 in which the strong electro-negative and electro-positive zones were identified and along with vector symmetry. The entire structure was constructed by coordinate covalent bond as expected and the negative and positive boundary regions were defined according to the Mulliken charge reorientation. Here, the material was formed by negative O and positive Ag. Even though, both the atoms having bivalence, the formation of molecular orbitals purposively changed the polarity of atoms. This creates strong dipole bonds among the atoms which causing the well-built FCC structure. Usually, the charge separation in the molecule is purposively made by chemical equilibrium forces existed among the molecular lattice. Here, it was manifested by molecular dipoles in the material site. And it causing for the faithful physico-chemical property. Hence, since it was well arranged on molecular site, the Ag nano material fascinated by O vacancies which was found to be effective for the inducement of semi-optical and physico-chemical properties.

3.3. STRUCTURE DEFORMATION ANALYSIS

TABLE 2
OPTICAL PARAMETERS OF Ag_2O THIN FILMS AT DIFFERENT TEMPERATURE

Annealing temp in ° C	Refractive index	Band gap (eV)	Extinction coefficient	Absorption Coefficient	Particle size(nm)	ε_1 n^2-k^2	ε_2 2nk
Room temperature	2.233	-	4.6140	0.462×10^{-5}	-	4.221	2.751
100	2.274	1.513	5.237	1.421×10^{-5}	31.52	4.88	2.374
200	2.296	1.545	6.088	0.272×10^{-5}	37.54	4.869	2.804
300	2.323	1.571	6.102	0.241×10^{-5}	42.25	5.016	2.872

The optimized parameters of the crystal structure in different annealing temperatures were depicted in the Table 2. The annealing effect was observed in the form of variation in bond length and bond angle of the crystal molecular structure. At 100º C, the bond length of Ag and O was determined to be 2.2773Å and it was slightly varied at 200º C which found to be 2.2391Å. In addition to that, at 300ºC, the same bond length was determined to be 2.1990 º. From this result, it was concluded that, the entire optimized parameters associated bond lengths and bond angles were reduced by the application of temperature and at high temperature; the bend length was considerably decreased. Such a change of parameters caused to the generation of spontaneous physical strain as well as the decrement of particle size. The bond length of Ag-O was observed differently with respect to the position of bond in the crystal structure. Such as Ag1-O5, Ag2-O4, Ag2-O5 and Ag2-O11 were determined to be 2.773Å, 2.240Å, 1.195Å and 2.851Å respectively. The modified bond length between the silver and O atoms was differed from 0.045 Å to 0656 Å in the molecular site. From the observed fluctuated bond length, it was conferred that, the architecture of FCC lattice in the present prepared nano material was found to be rather distorted in the shape. This was mainly due to the interstitial substitutions of O in the molecular site.

3.4. FRONTIER MOLECULAR ORBITAL SUPPORT

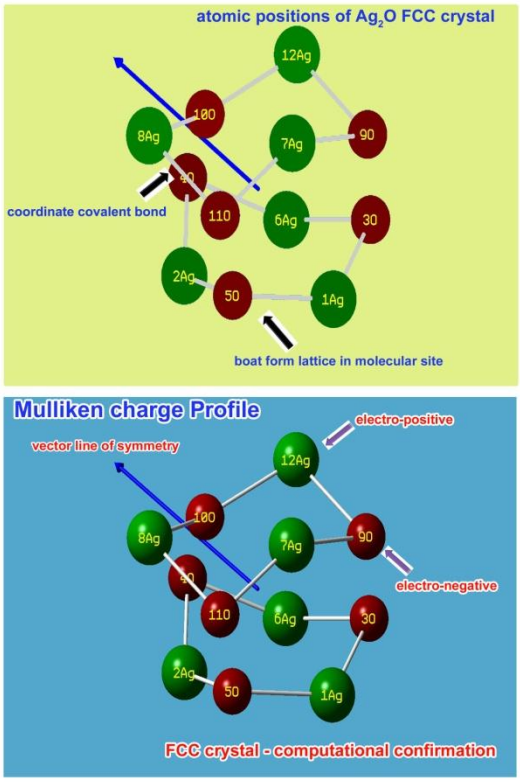

FIGURE 7
MOLECULAR INTERACTION PROFILE OF Ag_2O NANO MATERIAL

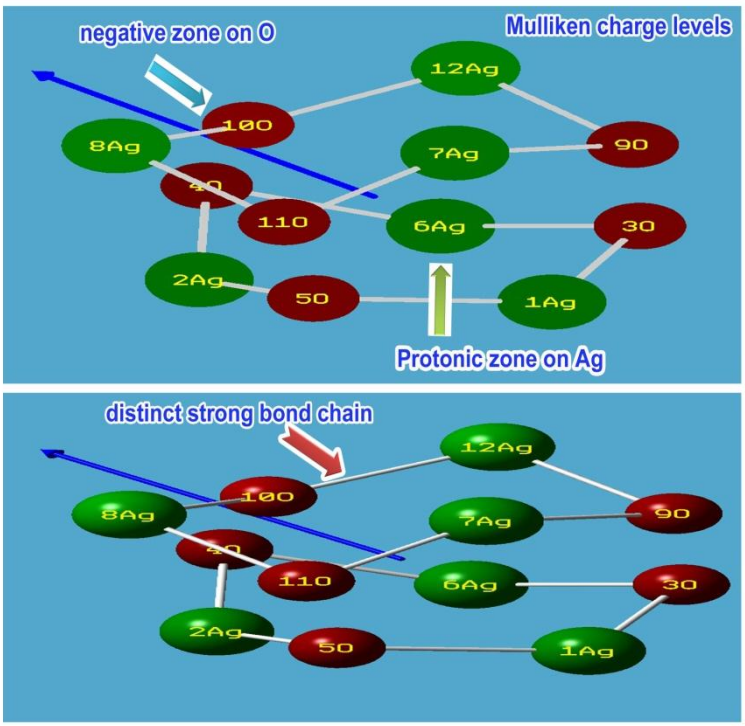

The molecular interaction profile of Ag_2O nano material was displayed in the Figure 7 where in which the molecular interactions were taking place among the molecular orbital segments. Here, in the case of LUMO, the orbital overlapping taking place by space orbital polarization which was appeared over Ag to Ag atoms via O atom. This spatial quantization profile was found to be ready to occupy the energy which was from HOMO interaction contour. Only one covalent bond was appeared in the structure which showed the center of symmetry of crystal. When compared with blown orbital interaction, very feeble orbital interactions come into sight for receiving the transitions from occupied energy levels.

In the case of HOMO, the dumbbell shaped occupied coordinate covalent interactions were arranged to blend the degenerate electronic energy for radiating electronic energy to the unoccupied energy levels. In HOMO-1, the molecular orbitals linked the Ag atoms with the O by interconnecting the degenerate orbitals in which the electrons with different quantized energy can be moved in force field and this setup usually able to receive optical energy in wide range of spectral region and capable of restoring the energy. In LUMO+1, the space interactions were increased in blown orbital arrangement. Two sets of iso blown system of resultant Ag dipole was extended over the crystal as a whole which forms consistent nano crystal with sufficient quality profile. The cascade from of orbital interaction settled up in similar coordinate atoms by which the material is able to control the optical route for harmonic waves which was entered in to the material. Thus, the Ag_2O nano material can be used to fabricate the multifunctional opto-electronic as well as photo-voltaic devices.

3.4. MEP FORMATION ANALYSIS

The electronic stability of the nano material was established by the depletion of electrophilic and nucleophilic regions that are usually architected by molecular charge displacement over the molecule. The electrophilic region and nucleophilic region was appeared on O and Ag atoms respectively in the crystal site and the moderate region was found in between the atoms. The centripetal static field was found to be focused on Ag and centrifugal dynamic field was appeared to be on O atoms. This array of Ag_2O nano particles in different planes shaped closed morphological surface and it framed the FCC crystal consistently.

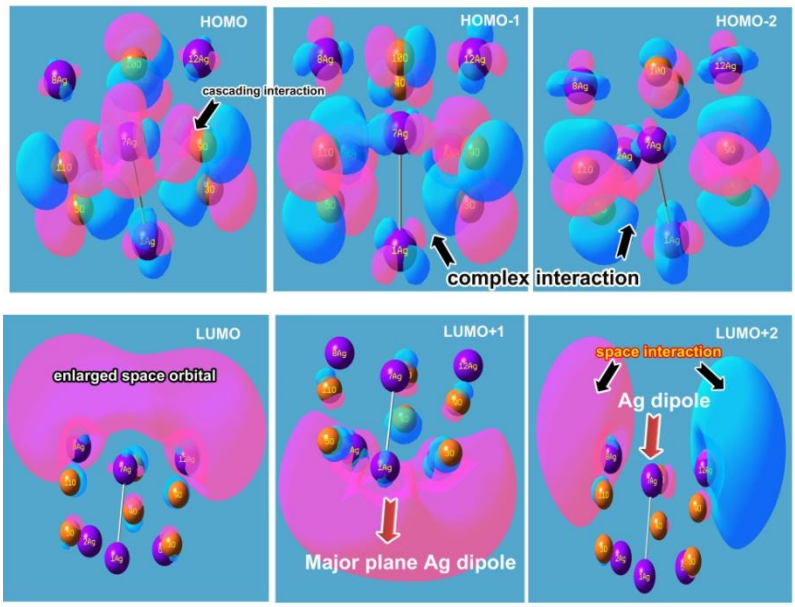

FIGURE 9
ENERGY DISTRIBUTION OF ELECTRONIC POTENTIAL CONTOUR

The MEP diagram and energy distribution of electronic potential contour was shown in Figure 9. The finger print of static field distribution was displayed in which the centripetal potential field of Ag was found to be spread out from the crystal and centrifugal static field supporting the dynamic potential. This setup in the nano material making the path is able to have enriched pathway to accelerate the electronic energy by drifting potential in the crystal site.

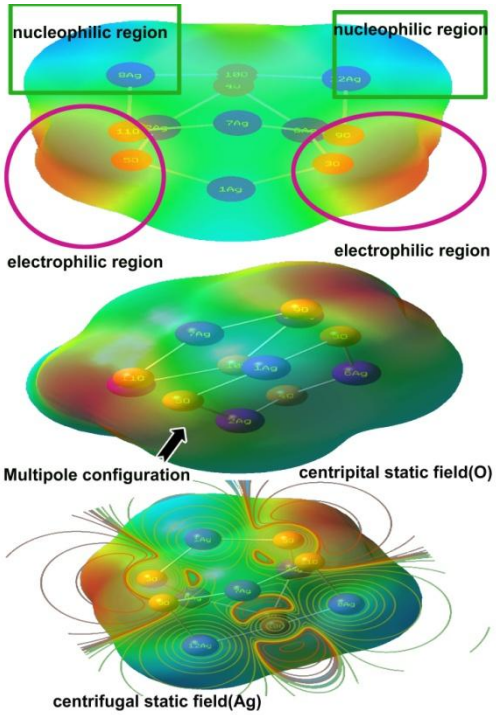

4. CONCLUSION

The Ag_2O nano material was prepared by well defined method of synthesize and it was characterized by experimental as well as theoretical tools. The effect of annealing temperature to improve the crystal quality and multifunctional character of the material was discussed. The important morphological, electronic and optical parameters were calculated and evaluated to study the characteristics of the materials. The recurrence of multidimensional Ag_2O array by the application of

annealing temperatures and thereby the assembly of microstrain produced in the crystal was keenly observed and examined. The change of Ag_2O reciprocity by the effect of thermal strain was studied for examining the material application. The molecular orbital interaction causing the optical characteristics was thoroughly investigated and the resultant application was determined.

REFERENCES

1. D. M. Bailey, Acta Crystallography, 23, (1967), 729.
2. Caue Ribeiro, Edson Roberto Leite, Crystallization and Growth of Colloidal Nanocrystals, Springer publications, vol. 1, (2011).
3. Xiaogang Peng, Michael Mingos, Semiconductor Nanocrystals and Silicate Nanoparticles, Structure and bondings, Springer Berlin Heidelberg New York, (2005).
4. K. Bhattacharya, S. Conti, G. Zanzotto and J. Zimmer, Nature 428: (2004) 55.
5. X.Y. Gao, Z.Y. Zhang, J.M. Ma, J.X. Lu, J.H. Gu and S.E. Yang, Chinese Physics B, vol. 20, (2011) 026103-6.
6. X.Y. Gao, H.L. Feng, Z.Y. Zhang, J.M. Ma and J.X. Lu, Chinese Physics Letters, vol. 27, (2010) 026804.
7. L.A.A. Petersson and P.G. Snyder, Thin Solid Films, vol. 270, (1995) 69-72.
8. Maissel, L. I., and Clang, R., (eds.), Handbook of Thin Film Technology, McGraw-Hill, New York (1970).
9. Bunshah, R. F., (ed), Deposition Technologies for Films and Coatings: Developments and Applications,Noyes Publications, Park Ridge, NJ (1982).
10. K. Kadau, T. C. Germann, P. S. Lomdahl, and B. L. Holian, Phys. Rev. B, 72: (2005) 064120.
11. Ng Law Yong, Akil Ahmad Ng Law Yong, , Abdul Wahab Mohammad, International Journal of Scientific & Engineering Research, Volume 4, Issue 5, (2013) 155-158.
12. A Bhattacharjee, M Ahmaruzzaman, T Sinha, Spectrochimica Acta Part A: Molecular and Biomolecular Spectroscopy 136, 751-760.
13. T Sinha, M Ahmaruzzaman, A Bhattacharjee, Journal of Environmental Chemical Engineering 2 (4), 2269-2279.
14. Pawel E. Tomaszewski, Phase Transitions, 1992, Vol. 38, pp. 127-220.
15. Marko V. Jaric, J. Math. Phys. 24 (12) (1983), 2865-2882.
16. M. Erol, Y. Han, S.K, Stanley, C.M. Stafford, H.Du, S. Sukhishvili, J.Am.Chem,Soc.2009, 131,7480.
17. Y. Hoshi, T. Kiyomura, Thin Solid Films 411 (2002) 36.